Non-lethal oxidative stress boosts bacterial survival and evolvability under lethal exposure

Alexandro Rodríguez-Rojas[1]*, Josh Kim[1], Paul Johnston[1], Olga Makarova[1], Murat Eravci[2], Christoph Weise[2], Regine Hengge[3] and Jens Rolff[1]*.

[1]Institut für Biologie, Freie Universität Berlin, Königin-Luise-Strasse 1-3, 14195 Berlin, Germany.

[2]Institut für Chemie und Biochemie, Freie Universität Berlin, Thielallee 63, 14195 Berlin, *Germany*.

[3]Institut für Biologie/Mikrobiologie, Humboldt-Universität zu Berlin, Philippstr. 13, 10115 Berlin, Germany.

*Correspondence authors: a.rojas@fu-berlin.de, jens.rolff@fu-berlin.de

Abstract

Oxygen accumulation by photosynthesis and its utilization for respiration shaped the earliest life forms. Reactive oxygen species such as hydrogen peroxide, a toxic by-product of aerobic respiration became a challenge. Still, multicellular orgarhenggea@zedat.fu-berlin.denisms began to employ reactive oxygen species as potent weapons against microbes. Albeit bacterial defences against oxidative stress have been studied in model bacteria, the role of prevalent fluctuating concentrations remain unexplored. Here, we show how sub-lethal exposure of E. coli to hydrogen peroxide results in enhanced survival of primed cells when they later face killing concentrations. The basis and the duration of the response (memory) were determined by time-lapse quantitative proteomics. A low level of peroxide induces several scavenging enzymes that are quite stable, protecting cells from future exposure. We then asked if the phenotypic resistance against H2O2 alters resistance evolution against oxygen stress. Experimental evolution for H2O2 resistance revealed faster evolution and reaches stronger resistance in primed cells. Several mutations were found involved in resistance of evolved populations affecting a different type of loci but counterintuitively, none of them was implicated in scavenging systems. Our results have implications for host colonisation and infections where microbes often encounter reactive oxygen species in gradients.

Introduction

The ability to solicit an improved stress response when encountering repeated stress relies on 'remembering' a similar event from the past (memory) and is common to many biological entities. Stress sensor systems can prime organismic stress [1]. Bacteria encounter increasing and repeated stress imposed by the host immune system, during the cause of an infection or the colonization of a gut [2,3]. Obata et al, for example, recently demonstrated that low levels of hydrogen peroxide (H_2O_2) in the gut of *Drosophila melanogaster* shape the composition of the gut microbiota resulting in differential survival of the flies [3]. Here, we report how bacteria respond to low levels of ROS exposure and how this impacts bacterial fitness. We then investigate if the phenotypic response to a sub-lethal dose of H_2O_2 facilitates resistance evolution, hence providing a test of the phenotype-first hypothesis [4].

In *Escherichia coli*, the defences against oxidative stress depend on transcriptional regulators such as OxyR or SoxR that detect different changes in the redox balance and induce the production of detoxifying enzymes [2]. Oxidation of OxyR by hydrogen peroxide (H_2O_2) leads to the formation of an intra-molecular disulfide bond between cysteine residues 199 and 208 and OxyR is deactivated by enzymatic reduction with glutaredoxin I or thioredoxin. OxyR positively regulates catalases and peroxidases. Because also Grx and GorA are transcriptionally regulated by OxyR, the whole response is autoregulated [5].

The OxyR-mediated oxidative stress response results in scavenging of H_2O_2 and hence mitigates the toxicity of this by-product of aerobic metabolism. This includes the induction of the Suf proteins that form a complex to supply apo-enzymes with iron-sulfur clusters. This system replaces the Isc system, which is disrupted by H_2O_2 stress [6,7]. The iron sulphur clusters of dehydratases are one of the most H_2O_2-sensitive systems. The repair of these clusters by Suf is necessary to prevent the failure of the TCA cycle. The iron-sulfur clusters are enzymes that employ ferrous iron as a co-factor that can increase the risk of fuelling a Fenton reaction. The nucleoid-binding protein Dps binds intracellular

free iron to limit the generation of hydroxyl radical close to the vulnerable DNA [8].

In a classic paper it has been shown that the pre-treatment with a low dose (60 µM) of hydrogen peroxide can increase *E. coli* survival of immediate exposure to a highly lethal dose (30 mM) [9]. However, neither the duration of such priming responses nor the molecular mechanisms of the memory have been studied. Our study has two main aims. First, we want to investigate the main players in the H_2O_2 priming response and for how long the response is sustained. Second, we want to used this system to test the hypothesis that inducible phenotypes accelerate adaptive evolution. Therefor we experimentally evolved *Escherichia coli* under a growing level of Hydrogen peroxide with and without priming (warning). For H_2O_2-resistant populations under priming and non-priming regimes, genome re-sequencing analyses were performed to identify involved mutations. We focus our study on growing bacteria (exponential phase), as this better reflects the situations during an infection or colonisation of host surfaces including the gut.

Results and discussion

Priming by H_2O_2 results in higher bacterial survival

We find that the minimal inhibitory concentration for hydrogen peroxide is 1 mM and find a clear dose-effect in survival rate (figure 1a, ranging from 50 µM to 1 mM, figure 1a, $p=2.1x10^{-16}$, DRC model fitted based on maximum likelihood [10]). Based on these results we then primed cells with H_2O_2 0.1 mM, the maximum concentration that shows no difference in growth rate compared to non-treated cells, and monitored survival at minimal inhibitory concentration, 1 mM starting half an hour after removal the treatment. Primed (pretreated) populations of *E. coli* showed higher survival than naïve cells by more than one order of magnitude (Cox proportional hazard model, $p<0.05$, figure 1b).

These results are in agreement with data previously reported by Imlay et al [9], showing survival protection even to doses as high as 30 mM, a concentration close to hydrogen peroxide usage as disinfectant. Our concentrations are in the range of some *in vivo* situations. For example, tailfin transection on zebrafish larvae induce rapid increase in H_2O_2 levels ranging from 100–200 µM in the wound margins [2]. In some cases more than 100 µM of H_2O_2 have been reported in human and other animal aqueous and vitreous humors of the eye [11]. We investigated additional concentration ranges, using a plate reader at higher cell density, indicating that priming response occurs at different concentrations and cell densities (figure S1).

Duration of the priming response

As the priming response protects the cells effectively from lethal exposure to H_2O_2, an important question is for how long this response remains effective? To address this, we repeated the first experiment, but applied a trigger concentration (1 mM) at different times-points (60, 90, 120 and 150 minutes after priming, at constant cell density. We observed a significant decay of the priming response from 120 minutes after H_2O_2 pre-treatment removal (figure 2), roughly four divisions (inferred from optical density values, figure S3), suggesting that the priming effect is also trans-generational. After 150 minutes, the survival rate of priming populations did not differ from naïve ones anymore. Another study has shown long-term memory based on epigenetic switch able to control a bimodal virulence alternation also in the scale of hours in *E. coli* [12]. Similarly, the presence of a long-retention effect, or “memory effect,” of the persister cell state has been also described for *E. coli* and a wide variety of other bacteria [13].

How is the state of priming maintained for so long? Bacteria can store information from recent stress via stable transcripts or proteins [14,15]. We investigated the memory at the protein level and initially studied the impact of the two concentrations used across most of our experiments (0.1 and 1 mM) on the proteome of *E. coli* by quantitative LC-mass spectrometry. From the quantitative proteomic dataset, we detected many of the known enzymes that

are induced by hydrogen peroxide just five minutes after the addition of H_2O_2 (figures 3, and tables S2 and S3). For both concentrations, we detected and quantified many proteins under OxyR regulon.

To explore temporal dynamic of the proteome after 30 minute stimulus with H_2O_2 (0.1 mM), we followed the changes over almost three hours (five time points: 30, 60, 90, 120 and 150 minutes). The decline in anti-H_2O_2 protein levels correlates well with the decrease of the response (figure 4 and tables S4 and S4). Some important proteins such as KatG and AhpCF declined slowly, reflecting probably more a dilution by cell divisions than degradation, after removal of the H_2O_2. These results indicate that many of these proteins are stable and show a significantly higher abundance than in the control even at 150 minutes after H_2O_2 treatment. Other proteins such as GrxA, YaaA and XthA, SufA, SufS, AcrA-AcrB completely declined at this point indicating that these proteins may be subject to proteolysis or or have shorter half-life (figure 4) but also that the stressful situation is alleviated. The overall results of this proteomic experiment strongly suggest that the memory of priming response in *E. coli* is mediated by the scavenging proteins such as KatG and AhpCF or repairing proteins such as RecA.

To investigate the global impact of the priming concentration of H_2O2 we applied a network analysis based on protein-protein interaction. We observe a high degree of connectivity in network of protein-protein interaction of both fractions, up- and downregulated (figure 5). If we compare our network with a large-scale protein-protein interaction network of *E. coli* [16], we fined that some of the most important nodes such as the general chaperons GloL (down-regulated) and DnaK (up-regulated) are affected. Other important global regulators such as Crp protein are overexpressed, indicating also an impact of H_2O_2 in the central metabolism. This analysis also suggests that there is a wide-proteome readjustment to cope with hydrogen peroxide stress that does not only involve scavenging systems and but shows a profound impact of oxidative stress across the entire proteome in a dose that does not change the growth rate in a rich medium.

Another contributing factor to memory could be based on stable transcripts. Thus, we sequenced the full transcriptome after exposure to H_2O_2. RNAseq capturing both sRNA and mRNA, sampling just before the decline of the response (120 minutes after the stimulus, figure S3). The highest expressed transcript was OxyS, a small regulatory RNA (sRNA) induced by active OxyR (figure S3, to see full results in tables S4 and S5). OxyS regulates several genes, and although several targets have been identified, its function is not fully understood [17]. We did not detect other transcripts related to the OxyR regulon.

OxyS is a potential candidate to explain the duration of priming because it is relatively stable with a half-life between 18 to 20 minutes during the exponential phase [18–20]. To explore this, we used an *oxyS*-deficient mutant to test its susceptibility to H_2O_2 over 30 minutes. We did not find any significant difference in susceptibility consistent with prior reports [19,21,22]. Although OxyS did not provide us with a mechanism to explain the duration of the memory, its stability could play some role in alleviating DNA damage as recently suggested [23]. However, such protection does not seem to have a significant impact on survival, according to our results.

We detected most of the known genes under OxyR regulation. We also found that the capacity of the cells 'to remember' the stimulus is mainly based on the long life of scavenging proteins as documented in the proteomic data, that after synthesis remain up as long as 120 minutes after removal of peroxide. It is possible than many of these enzymes are not degraded but just simply diluted as cell divisions goes by explaining the pattern that we observe in the decline of the response.

Priming response is compromised by disrupting important H_2O_2-scavenging genes

Since hydrogen peroxide response is well studied in *E. coli*, we first checked that our priming concentration was inducing an anti-H_2O_2 response. The expression of important genes for H_2O_2 stress survival were analysed by qPCR

30 minutes after the addition of H_2O_2 (0.1 mM). H_2O_2 induced a significant up-regulation of representative genes such as *katG*, *ahpF*/*ahpC*, *dps*, *mntH* and *sufA* (figure S2 and table S1). The coding gene for the regulator OxyR was not differentially expressed, indicating that there is no stimulation of OxyR transcription under H_2O_2 stress. It is known that the path for the activation of OxyR leads to the formation of an intra-molecular disulfide bond between cysteine residues 199 and 208. This means that OxyR is a sensor of intracellular redox status and becomes active only when the intra-molecular disulfide bond are formed [5]. In in the line with previous works our results also show that OxyR translational response to hydrogen peroxide is not differentially changed [24]. We found also that Fur protein, a regulator of iron-import proteins is not differentially expressed in *E. coli*. It was expected that Fur level would be induced by hydrogen peroxide to decrease the amount of iron-importing transporters to decrease intracellular Fenton reactions [24]. Our experiments were carried out in LB, a medium that is iron-rich [25,26]. High level of iron represses the expression of iron-import proteins [27] and this is perhaps the reason why we did not detect changes at the transcription level of *fur* gene. Another difference with early studies is that the cell density in our experiments is kept low and eventually it would also decrease the influence of the cells on the concentration of both iron and H_2O_2 in the medium.

To understand the relevant molecular players in the priming response to H_2O_2, we constructed a set of mutants for the coding gene of key proteins that we found in our proteomic dataset. In proliferating *E. coli*, OxyR is the major regulator controlling cellular response to H_2O_2 [28]. We explored the involvement of OxyR in the priming response because many of the upregulated detected proteins are under this regulator. We found that by disrupting OxyR, there was a dramatic change in sensitivity with full loss of viability after 30 minutes (figure 6). The priming response is completely abolished (Figure 7), indicating that the enhanced survival due to pre-exposure to H_2O_2 depends on OxyR. OxyR is a fundamental transcription factor, probably the most important one, that protects *E. coli* against H_2O_2 during the exponential phase [28,29]. The active form of OxyR positively regulates dozens of genes. Next, we selected, from the highest expressed proteins, many from the OxyR, regulon, to determine which ones contribute more significantly to survival (figure 6) and

priming (figure 7). Removal of KatG (catalase), AhpF (subunit of the alkyl perxidase) or RecA (DNA repair) significantly decreases survival against hydrogen peroxide (1 mM). The double mutant for KatG/AhpF showed even stronger sensitivity. However, other important proteins induced by H_2O_2 such as YaaA (decreasses intracellular iron [30]), LipA (lipoate synthase, important for the repair of iron-sulfur clusters [31]), GltD (glutamate synthase subunit), GhxA or GhrA did not show differential survival to 1 mM concentration. The OxyS sRNA was the transcript with the highest level of expression in the RNAseq data, but the mutant did not display any susceptibility to H_2O_2 . Assuming that H_2O_2 sensitivity and priming response are closely linked, we included in the additional priming response experiment mostly those genes with increased susceptibility (figure 7). The removal of KatG indicates that catalase importantly contributes to priming response but it does not fully explain the protection observed for the WT strain. In the case of AhpF, we also observe differences in priming response with the naïve state but not that pronounced as the case of KatG deficient strain. The double mutant defective in KatG and AhpF showed a dramatic decrease in priming response but still significantly different from the naïve. Another protein that illustrates an important influence on priming response is RecA, which mutant show a decreased priming response to H_2O_2. OxyS mutant is not suppressive for priming response, indicating that its presence contributes neither to the survival or priming.

Priming response enhances the survival of evolving populations

Whether the priming response described above has an influence on the rate of evolution bacteria against hydrogen peroxide was the goal of the following experiments. We evolved bacterial cultures with a treatment protocol described in detail in M&M section. The idea was to evolve parallel populations where one group periodically is exposed to a sub-lethal concentration of hydrogen peroxide, an activating signal that should protect the populations in comparison with naïve ones when later exposed to a higher dose. We continued daily intermittent exposures to hydrogen peroxide doubling both, priming and triggering concentration until extinction is reached. We observe that extinction rate is faster for the naïve populations in comparison to primed ones (Log-rank test, $p < 0.05$), figure 8). Naïve cells evolved resistance of up

8mM H_2O_2, primed cells evolved resistance to at least 16mM H_2O_2This first results indicate that priming potentially increases evolvability of pre-treated populations.

Further analysis of the resistant populations by whole-genome sequencing revealed that all populations harboured different set of mutations. Surprisingly, we did not find any modification in the enzymatic scavenger systems, such as catalases, superoxide dismutases or any other under OxyR regulation. We found several hundred of single nucleotide polymorphisms (SNPs) and other type of mutations that were unique to each population for both regimes (figure 9). These mutations probably represent many of the neutral or non-lethal changes that populations accumulated during the exposure to H_2O_2, that is not simply a selector agent, but it also speeds up evolution by increasing the mutation rate. At the moment we cannot be certain that among these mutations we may find adaptive mutations. For example, a set of changes are located in genes coding for iron binding proteins or related with iron transport such as iceT, feoA, yaaX/yaaA or rsxC. The control of intracellular iron is crucial to decrease the adverse effects of Fenton chemistry [6].

There was also a set of more frequent changes that were common to both type of populations, evolved under priming and non-priming conditions (figure 9). The most important ones frequent mutations were yodB (a cytochrome b561 homolog), intergenic mutations between insA and uspC (universal stress protein C), intergenic mutations between flhD and insB1. Another frequent mutation was in the gene YagH, belonging to the CP4-6 prophage. CP4-6 is a cryptic prophage in *E. coli* that has been suggested could play a role in bacterial survival under adverse environmental conditions [32].

Priming alters the mutational spectrum and H_2O_2-induced mutagenesis in evolving populations

To assess if the evolved populations have a similar mutation spectrum, we analysed the total pool of mutations segregated by the treatments and determined the proportion of every type of found mutation. We used Monte

Carlo hypergeometric test implemented by iMARS [33], to assess the overall differences between mutational spectra. Both groups, of the evolving populations under priming and non-priming conditions, differed significantly (p=0.00021, figure 6). ROS induces a particular type of mutations, with a characteristic signature in the DNA. The guanine base in genomic DNA is highly susceptible to oxidative stress due to having the lowest oxidation potential. Therefore, G·C→T·A and G·C→C·G transversion mutations frequently occur under oxidative conditions [34,35]. Thus, we investigated the proportion of C→A and C→G substitutions between the two types of evolving regimes, but we did not find significant differences (p=0.056 and p=0.11 respectively, two-tailed Fisher's exact-test, figure 10).

A possible explanation for these results is that the pre-activation of antioxidant defences helps to decrease the number of non-adaptive mutations and lethality by decreasing the extend of the Fenton reaction. We observed an increase in the frequency of substitutions G→A, T→C, G→C, T→G and A→G in naïve populations compared to primed populations, suggesting that the primed cells have DNA-damage control. Primed populations showed an increase in frameshift mutations by deletion of 1 bp, and additions of C or G; these last two were only present in primed populations that also showed higher number of A→C substitutions.

It is expected that priming response would decrease DNA damage and hence also the lethal ones. To assess this possibility we tested if priming is able to decrease the mutant frequency and hence lethality due to mutagenesis. Preserving the conditions of the previous experiments, we treated the bacterial cultures with the same priming and triggering concentrations at low cell density. We found a decrease of more than one order of magnitude in mutagenesis while comparing H_2O_2-induced mutant frequency of in naïve and primed cultures (figure S4). This difference is significant since there is no overlapping for the confidence intervals of 0.95 ($3.2x10^{-7}$ to $4.92x10^{-7}$ for naïve and $1.75x10^{-8}$ to $5.62x10^{-8}$ for primed cells [36]). In our experiment, naïve and primed population showed differential death rate (figure 1). Recently, it has been suggested that antimicrobial induced mutagenesis could be influenced by death rate, related with population dynamics, however, the same study

concluded that this is not the case for hydrogen peroxide [37]. We also showed previously that different inoculum size on similar conditions to our experiment has no influence on mutagenesis [38]. This experiment allows us to deduce that one of the most important consequences of priming response to H_2O_2 is the drastic decrease of lethal mutagenesis, indicating that although hydrogen peroxide damage most of the cellular components [6], is DNA damage probably the one that contributes the most to lethality.

In principle, an increase of mutation rate is a parameter that increases the evolvability of asexual populations [39–41]. How is possible that naïve populations show lower evolvability compared to the primed ones if the mutagenesis is higher in the former ones? A possible explanation is that evolvability is also influenced by the population size and the mutation supply that is increased by mutagenesis balanced by the decrease in population size of the naïve population. We also found that the mutational spectra of our evolving populations are different. Mutational spectra, as a qualitative property of mutation rate that could enhance or hinder the access to beneficial mutations [42–44].

Conclusions

We found that priming by hydrogen peroxide is quantitatively driven by genes mostly under OxyR control. The memory can last up to four generations upon first exposure to H_2O_2 taking into account the time after addition of the stressor and number of divisions. We also determined for the first time the stability of hydrogen peroxide detoxifying proteins for the first time and found a long half-life which play a significant role on survival. We also show that priming plays a role in evolving populations enhancing the survival under oxidative stress supporting a link between phenotype as a target of selection during evolution processes providing a validation for the phenotype first hypothesis. The type and numbers of mutations indicates that scavenger system against oxidative stress are optimally evolved since no mutations affecting these systems were found. Understanding the molecular basis of this enhanced resistance to oxidative stress in bacteria will almost certainly inform more effective intervention strategies in infectious diseases management. Our work also

contributes to understand how the adaptation of early life with oxygen could take place.

Material and methods

Bacteria and growth conditions. The *E. coli* MG1655 was used as bacterial model for all experiments with hydrogen peroxide. For genetic manipulation, *Escherichia coli* DH5α strain was used and routinely cultured in Lysogeny Broth (LB medium), supplemented with antibiotics when appropriate. All bacterial strains were cultured in Lysogeny broth lenox (Carl Roth, Germany). For all experiments with hydrogen peroxide the LB was fresh prepared and kept in the dark until use.

Construction and verification of deletion mutants. All mutants used in this work (table 3) were generated in *E. coli* K-12 strain MG1655 following the methodology described elsewhere [45]. Briefly, transformants carrying a red recombinase helper plasmid, pKD46, were grown in 5-ml SOB medium with ampicillin (100 µg/ml) and L-arabinose at 30°C to an O.D.600 of ~0.5 and then made electrocompetent. PCR products with homology regions were generated using specific primers (table 2). The PRC-generated fragments were gel-purified, digested with restriction enzyme DpnI to remove any traces of the antibiotic cassette donor plasmid (pKD3), column purified (MinElute PCR Purification Kit, Qiagen). Competent cells in 50 µl aliquots were electroporated with 100 ng of PCR product. Cells were added immediately 0.9 ml of SOC, incubated 1 h at 37°C, and then 100 µl aliquots spread onto LB agar with kanamycin (30 µg/ml). The correct inactivation of genes were verified by PCR.

Hydrogen peroxide susceptibility testing. When working with hydrogen peroxide, we carried out all the experiments with fresh-made LB to avoid the accumulation of chemically formed H_2O_2 by joined the action of light and flavin present in the medium during storage. Susceptibility to H_2O_2 was determined by exposing exponentially phase bacteria at a density of ~ $2x10^7$ CFU/ml to different concentrations and times, taking as a reference previous works.

Priming experiments with H_2O_2. Starting from $2x10^7$ CFU/ml, where *E. coli* the bacteria were exposed (stimulus) to 0.1 mM of hydrogen peroxide during 30 minutes at at 37°C with shaking. Catalase was added to a final concentration of 4 µl/ml, centrifuged at 4000 g during 10 minutes and allow to recover during 90 minutes, keeping the cell density constant by removing the needed volume and replace it with appropriate amount of fresh LB every 30 minutes. The trigger (H_2O_2 1 mM) was added 90 minutes after removal the stimulus. The challenge lasted for 30 minutes. At this point catalase (4 µl/ml) was added and cultures were diluted and plated to determine cell viability. Non treated cells were used as control. Five cultures per group were used.

Priming experiments in multi-well plates. The 96-multiwell plates were prepared under aseptic conditions. All experiments were carried out in a final volume of 100 µL of fresh LB. Bacteria were exposed to serially diluted concentrations of H_2O_2 from 256 mM by adding 50 µL of peroxide containing LB first 50 µL of mid-exponential phase bacteria rendering approximately 10^7 CFU/ml suspension. The plate was placed into a Synergy H1 plate reader (BioTek, USA) and kinetics of killing or growth were followed during two hours. Once those relevant non-lethal concentrations in these conditions were established, a second experiment was carried out. In a similar plate and conditions, bacteria were exposed to serial dilutions of H_2O_2 starting from 4 mM during 30 minutes. The plate was centrifuged, the supernatant removed and fresh LB transferred. The cells were allowed to recover for two hours. After this period, 50 µL were removed per well and replaced with 50 µL LB containing 32 mM of H_2O_2 for a final concentration of 16 mM. The killing and survival were followed for 8 hours by absorbance at 600 nm.

Memory of the priming response. After applying a stimulus (0.1 mM H_2O_2) during half an hour, the cells were allowed to recover for 30, 60, 90, 120 and 150 minutes before the addition of the trigger (1 mM H_2O_2). During the experiment, the D.O.600 of all cultures were kept around 0.05 by adding suitable volume and removal of equivalent quantity to maintain the population in exponential phase and the same population size. Bacteria remained exposed to the trigger during 30 minutes before starting the dilution in 1 ml of LB

452 containing 4 µg of catalase (Sigma-Aldrich, Germany). Appropriated dilutions
453 were made and plated onto LB agar to determine the survival rate.
454
455 **Global proteomics by mass spectrometry.** *E. coli* strain MG1655 was grown
456 at 37°C in LB medium to OD600 0.5. The cultures were diluted ten times in
457 fresh LB. H_2O_2 was added to tubes at 0.1 and 1 mM. Non treated samples were
458 used as control. All tubes were incubated during five minutes with shaking at
459 37°C. Remaining hydrogen peroxide was removed by adding 4 µg/ml of
460 catalase first and by centrifugation at 10000 g during 2 minutes. After removal
461 of the supernatant, equivalent amounts of fresh LB was added. For the memory
462 decline experiment, the procedure was identical, except that only 0.1 mM of
463 hydrogen peroxide was used and the samples were treated during 30 minutes.
464 After removal of the treatment, time-point samples were taken after 30, 60, 90,
465 120 and 150 minutes. Each experimental condition consisted of six replica. Two
466 millilitres per sample were pelleted by centrifugation at 10000 g for 2 minutes.
467 The cells were re-suspended in 50 ml of TE (10 mM Tris-HCl pH 8.0, 1 mM EDTA)
468 that contained chicken lysozyme (1 mg/ml, Sigma) and DTT (10 mM) and
469 incubated at room temperature for five minutes with occasional swirling. 250 µl
470 of denaturation buffer (6M urea/2 M thiourea in 10 mM HEPES pH 8.0) were
471 added into each sample. 10 µl (which approximately corresponds to 50 µg of
472 protein) of the resulting lysate were mixed with 150 µl of the denaturation
473 buffer and used for in-solution protein digestion as described previously [46].
474 Briefly, proteins, demobilised in denaturation buffer, were reduced by addition
475 of 1 ml of 10 mM DTT dissolved in 50 mM ammonium bicarbonate (ABC) and
476 incubation for 30 minutes, followed by alkylation with 1 µl of 55 mM
477 iodacetamid dissolved in 50 mM ABC for 20 minutes, digestion with 1 µg Lysyl
478 endopeptidase (LysC, Wako, Japan), resuspended in 50 mM ABC, for 3 hours.
479 After pre-digestion with LysC, protein samples were diluted four times with 50
480 mM ABC and subjected to overnight trypsin digestion using 1 µg of sequencing
481 grade modified trypsin, Promega), diluted in 50 mM ABC. All in-solution protein
482 digestion steps were performed at room temperature and after addition of
483 iodacetamid the samples were protected from the light until the digestion was
484 stopped by adding 10 ml of Buffer A* (5% acetonitrile, 3% trifluoric acid). After
485 trypsin digestion overnight at room temperature, samples were diluted with
486 200 µl of buffer A (5% acetonitrile, 3% trifluoracetic acid) treated as

487 described elsewhere and vacuum dried. Re-dissolved samples were loaded on
488 a ReprosilPur C18 reverse phase column and peptides were analyzed using a
489 nano-HPLC Dionex Ultimate 3000 system (Thermo scientific) coupled to an
490 Orbitrap Velos mass spectrometer (Thermo scientific). MS and MS/MS data from
491 each LC/MS run were analyzed with MaxQuant software (Version 1.3.0.5.) [47].
492 Identification of proteins was performed using the MaxQuant implemented
493 Andromeda peptide search engine.
494
495 **Quantification of gene expression.** To assess the quality of hydrogen
496 peroxide stress response related genes in *E. coli*, treated bacteria comparison
497 with 0.1 mM of hydrogen peroxide were compared to non-treated control.
498 Preparation of each of the six treatments and the control samples was carried
499 out by two operators three times on three consecutive days, thereby
500 comprising three biological replicates for each of the six experimental and one
501 control groups. Overnight (ON) cultures were diluted 1:100 in fresh LB,
502 subdivided into six 10 ml aliquots and incubated in 50 ml-Falcon tubes at 37°C
503 for 2.5 hours at 220 rpm. When the OD600 of bacterial cultures reached 0.4-
504 0.5, the cultures were diluted ten times with LB and hydrogen peroxide was
505 added to the final concentrations of 0.1 mM. These bacterial cultures were
506 incubated for 30 minutes at 37°C with shaking. Catalase was added to each
507 tube to a final concentration of 4 µg/ml. Ten millilitres of treated cultures and
508 from the control tubes were collected, immediately centrifuged at 10 000 g for
509 2 minutes and the supernatant was fully removed. The bacterial pellets were
510 resuspended in 1 ml LB, followed by addition of 1ml of RNAprotect Bacteria
511 Reagent (Qiagen, Germany), incubated during 2 minutes and centrifuged at
512 10000 g for 2 minutes at room temperature. The supernatant was discarded
513 and the bacterial pellet was immediately frozen and stored at -80°C until RNA
514 extraction.
515
516 RNA was isolated using RNeasy kit (Qiagen) according to the manufacturer's
517 instructions and eluted in 50 µl of RNase-free water. The nucleic acid yield and
518 purity were determined by measuring the optical density at A260/280 using
519 Nanodrop spectrophotometer (Thermo Scientific). RNA samples were treated
520 with TURBO DNase (Life Technologies). Briefly, 10 µg of RNA were used in a
521 total volume of 500 µl containing 20 units of TURBO DNase, incubated for 30

522 minutes at 37°C, immediately followed by RNeasy (Qiagen) clean-up and
523 elution in 30 µl of RNase-free water. Following DNase treatment, RNA integrity
524 was assessed using Agilent RNA 6000 Nano kit and 2100 Bioanalyzer
525 instrument (both Agilent Technologies). All samples had RIN values above 8.
526
527 For cDNA synthesis, total RNA (250 ng per reaction) and random primers were
528 used for cDNA synthesis using High-Capacity cDNA Reverse Transcription Kit
529 with RNase Inhibitor (Applied Biosystems). Initially, to ensure linear conversion
530 of the transcripts, the dynamic range of reverse transcription reaction was
531 tested by performing a standard curve with cDNA, synthesised using various
532 input amounts of pooled RNA. To obtain sufficient amount of cDNA, several
533 batches of 20 µl RT reactions were pooled, diluted 50-fold with RNase-free
534 water and stored in single-use aliquots at -80°C until further use. All 21
535 samples were tested for presence of contaminating genomic DNA by running
536 the mdoG assay with cDNA and the respective no reverse transcription (-RT)
537 controls. There was no amplification in the majority of –RT controls. In –RT
538 samples with detectable amplification, difference in Ct values when compared
539 with +RT varied between the samples, but was no less than 10 cycles for all of
540 them with the lowest Ct values in –RT control samples ≥ 30.
541
542 For primer design, *Escherichia coli* strain K-12 MG1655 complete genome
543 (accession U00096) sequence was downloaded from NCBI database
544 (www.ncbi.nlm.nih.gov) and used as reference. Target sequence accession
545 number, location of the amplicon, amplicon length and primer sequences for
546 each assay can be found in table AX. Primers were designed using Primer
547 Express software (Applied Biosystems) and optimized for annealing
548 temperature of 60°C. Each primer pair and amplicon were checked for
549 secondary structure formation using Oligo Tool (Integrated DNA technologies,
550 http://eu.idtdna.com/analyzer/Applications/OligoAnalyzer/).
551
552 Quantitative Real-time PCR reactions were prepared manually in a total volume
553 of 10 µl by mixing 5 µl 2x KAPA SYBR FAST ABI Prism master mix (KAPA
554 Biosystems), 0.2 µl forward and reverse primer mix (10 µM each primer), 2.8 µl
555 RNase-free water and 2 µl cDNA in MicroAmp Fast Optical 48-wells reaction
556 plates (Applied Biosystems). PCR reactions were run in the Fast mode using

StepOne thermocycler (Applied Biosystems) with the following cycling conditions: 95°C 3’ /40x(95°C 3’’/60°C 20’’)/melting curve analysis. Each assay was run in duplicate. No template controls (NTC) were run each time. Presence of a single specific product was verified by running a melt curve analysis followed by visualisation of the qPCR product in a 2% agarose gel stained with SYBR Safe DNA Gel stain (Life Tecnologies). Additionally, each PCR assay was tested for reaction efficiency as follows: equimolar amounts of cDNA from all 21 samples were pooled together and used for the preparation of the standard curve by serial dilution (1:3) over five dilution points and run in triplicate. Expression of target genes was normalized to the expression levels of three reference genes (*arcA*, *mdoG* and *tus*), selected based on the assessment of the expression stability across all experimental conditions using BestKeeper software. Reaction efficiency information inferred from the standard curve data was used to correct for differences in amplification efficiencies in the REST 2009 software [48]. Default settings (2000 iterations) were used for randomisation and bootstrapping analysis to test significance of gene expression. Expression values with p-values ≤0.05 were assigned as differentially expressed. The relative gene expression results can be found in supplementary table A4. We followed the Minimum Information for Publication of Quantitative Real-Time PCR experiments (MIQE) guidelines-compliant check-list [49].

For data analysis, qPCR Amplification curves were first visually examined in the StepOne software (Applied Biosystems). No baseline and threshold line adjustments were necessary. Ct values of the technical replicates were averaged and used for relative gene expression analysis in the REST 2009 software (Qiagen, Germany) [48]. Expression of target genes was normalized to the expression levels of three reference genes (*arcA*, *mdoG* and *tus*), selected based on the assessment of the expression stability across all experimental conditions using BestKeeper software. Reaction efficiency information inferred from the standard curve data was used to correct for differences in amplification efficiencies in the REST 2009 software. Default settings (2000 iterations) were used for randomisation and bootstrapping analysis to test significance of gene expression. Expression values with p-values ≤0.05 were assigned as differentially expressed. The relative gene expression results can

be found in supplementary table A4. We followed the Minimum Information for Publication of Quantitative Real-Time PCR experiments (MIQE) guidelines-compliant check-list [49].

Transcriptome sequencing. The transcriptome sequence was carried out on samples treated with 0.1 mM of hydrogen peroxide during the experiment of memory decline. The time point used corresponded to 120 minutes after removal of the treatment. Bacterial cells that were kept in low density (0.05 O.D.600) were concentrated ten times and the pellets were resuspended in 1 ml of lysis buffer. Both, small RNA fraction and the large one were isolated using the microRNA & small RNA Isolation kit (Thermo Fisher Scientific, Germany). Traces of genomic DNA were removed from 10 µg of RNA by digestion in a total volume of 500 µl containing 20 units of TURBO DNase, incubated for 30 minutes at 37°C, immediately followed by RNeasy (Qiagen) clean-up and elution in 30 µl of RNase-free water. Following DNase treatment, RNA integrity was assessed using Agilent RNA 6000 Nano kit and 2100 Bioanalyzer instrument (both Agilent Technologies, USA). Both fractions were depleted from ribosome RNA using the Ribo-Zero depletion Kit for Gram negative bacteria (Illumina, USA). Libraries were prepared using a TruSeq Stranded Total RNA library preparation kit (Illumina, USA) and were sequenced on a MiSeq platform. All sequences are available are available from the NCBI SRA under BioProject accession PRJNA485867.

Evolution experiment. Before the beginning of the experiment, five independent clones of *E. coli* MG1655 were pre-adapted to the experimental conditions such as culture medium, temperature and oxygen level and other parameters. The pre-adaptation were carried out by diluting an overnight culture of each clone 1:1000 and incubated at 37°C in the plate reader with the same shaking conditions used during the rest of the experiment in 0.2 ml in fresh-made Lysogeny Broth Lenox(LB). The bacteria we cultured by serial passage every 24 hours using a bottleneck of 1% (1/100 dilution) to allow for approximately fifty generations during ten days. Contamination checks by plating out on LB and cryopreservation of culture aliquots at -80°C in LB containing 15% glycerol solution were carried out periodically. All lines showed similar fitness and five independent colonies (one per line) were selected for

627 the evolution experiment. The experiment was performed at 37°C with
628 periodical shaking in a microplate reader (Synergy 2, Biotek). We used flat
629 bottom polypropylene non-binding 96-well plates from Greiner Bio-One GmbH
630 (Germany). The plates were covered with polystyrene lids with anti-evaporation
631 rings also from Greiner Bio-One GmbH. A final volume of 200 µl per well was
632 used. Growth curves were generated by taking measurements of OD600 every
633 20 minutes (preceded by a brief shaking of 5 seconds). Everyday, the
634 experiment consisted of two stages. Every morning a V-bottom plate containing
635 190 µl of LB was inoculated with 2 µl of overnight culture and incubated for two
636 hours to reach an OD between 0.2 to 0.6. At this point, 3 µl of LB containing the
637 corresponding priming concentration of H_2O_2 (for populations to be primed) or
638 only LB (control populations) were added to each well. The plate was then
639 incubated for 30 minutes, centrifuged and the supernatant removed using an
640 8-channel vacuum line provided of disposable tips. The pellets were
641 resuspended in 200 µl of fresh LB and 190 µl were transferred to a new flat-
642 bottom plate, allowed the cell to recover for 30 minutes at 37 °C and
643 challenged with a ten-fold higher concentration of the priming one. The dish
644 was located in the plate reader and the growth was followed as described
645 above during 20 hours. The serial passage started at 50µM of H_2O_2. Next day,
646 the procedure was identical by both, priming and challenging concentrations
647 were doubled to reach a final challenging concentration of 32 mM of H_2O_2
648 where all bacterial population went extinct. Besides, 10 µl of the remaining
649 cultures were added to 180 µl of sterile 0.9% NaCl and then serially diluted,
650 plated and inspected for contamination.
651
652 **DNA isolation.** Genomic DNA samples for whole genome sequencing were
653 isolated using in house method based on fast phenol:chloroform extraction,
654 removal od RNA and ethanol precipitation, capturing the DNA in paper filter as
655 previusly described. The DNA quantity and quality were estimated by
656 measuring the optical density at A260/280 using the Nanodrop
657 spectrophotometer (Thermo Scientific) and agarose gel electrophoresis.
658
659 **Genome re-sequencing.** We sequenced the total genomic DNA coming from
660 sixty populations from the evolution experiment, all from the previous passage
661 before extinction (20 evolved from priming regime, 20 from non-priming regime

662 and 20 control strains). TruSeq DNA PCR-free libraries were constructed
663 according to the manufacturers instructions and sequenced for 600 cycles
664 using a MiSeq at the Berlin Center for Genomics in Biodiversity Research.
665 Sequence data are available from the NCBI SRA under BioProject accession
666 PRJNA485867.
667
668 The haploid variant calling pipeline snippy [50] was used to identify mutations
669 in the selection lines. Snippy uses bwa [51] to align reads to the reference
670 genome and identifies variants in the resulting alignments using FreeBayes
671 [52]. All variants were independently verified using a second computational
672 pipeline, breseq [53].
673
674 **Determination of H_2O_2-induced mutagenesis.** This procedure was carried
675 out following similar protocols to previous studies with some modifications
676 [54,55]. Five independent cultures (5 ml each one) of *E. coli* MG1655 was
677 grown in fresh-made LB medium to an OD of ~0.2. At this point, each culture
678 was diluted 10 times (volume was increased to 50 ml) with LB and divided into
679 two separate sets of 25 ml per culture each one. One set, consisting of five
680 cultures of 25 ml was treated with 0.1 mM of H_2O_2 (primed) while the second
681 set of culture remained untreated (naïve). After 30 minutes, both cultures were
682 treated with 1 mM of H_2O_2 during another 30 minutes. Then, H_2O_2 was
683 removed, first, by quickly adding 4 µl/ml of catalase and, second, by collecting
684 the cells by centrifugation and washing them with one ml of fresh LB. For
685 determination of H_2O_2-induced mutation frequency, 4 ml of fresh LB was
686 inoculated with 1 ml of washed bacteria from each culture. The cultures were
687 allowed to recover overnight 16 h at 37°C. Serial dilutions of each culture were
688 plated next day onto LB plates containing 100 ug/ml of rifampicin or without
689 antibiotic to estimate the viability. The H_2O_2-induced mutation frequencies of
690 both, primed and naïve groups were calculated using the online tool FALCOR for
691 mutation rate estimation based on maximum likelihood [36].
692
693 **Statistical analysis.** All test were performed with software package R [56].
694

Funding information. ARR and JR were supported SFB 973 (Deutsche Forschungsgemeinschaft, CRC973, project C5) and OM and JR by European Research Council grant 260986 to JR.

Acknowledgements. We would like to thank Heidrun Häweker and Elisa Bitterman for help with library preparations and technical assistance.

References

1. Hilker M, Schwachtje J, Baier M, Balazadeh S, Bäurle I, et al. (2015) Priming and memory of stress responses in organisms lacking a nervous system. Biol Rev Camb Philos Soc. Available: http://www.ncbi.nlm.nih.gov/pubmed/26289992. Accessed 14 September 2015.
2. Wittmann C, Chockley P, Singh SK, Pase L, Lieschke GJ, et al. (2012) Hydrogen Peroxide in Inflammation: Messenger, Guide, and Assassin. Adv Hematol 2012: 1–6. Available: http://www.hindawi.com/journals/ah/2012/541471/. Accessed 28 July 2016.
3. Obata F, Fons CO, Gould AP (2018) Early-life exposure to low-dose oxidants can increase longevity via microbiome remodelling in Drosophila. Nat Commun 9: 975. Available: http://www.nature.com/articles/s41467-018-03070-w. Accessed 4 June 2018.
4. Levis NA, Pfennig DW (2016) Evaluating ‘Plasticity-First’ Evolution in Nature: Key Criteria and Empirical Approaches. Trends Ecol Evol 31: 563–574. Available: http://www.ncbi.nlm.nih.gov/pubmed/27067134. Accessed 4 June 2018.
5. Zheng M, Aslund F, Storz G (1998) Activation of the OxyR transcription factor by reversible disulfide bond formation. Science 279: 1718–1721. Available: http://www.ncbi.nlm.nih.gov/pubmed/9497290. Accessed 9 October 2016.
6. Imlay J a (2008) Cellular defenses against superoxide and hydrogen peroxide. Annu Rev Biochem 77: 755–776. Available: http://www.pubmedcentral.nih.gov/articlerender.fcgi?artid=3057177&tool=pmcentrez&rendertype=abstract. Accessed 2 May 2014.
7. Ezraty B, Vergnes A, Banzhaf M, Duverger Y, Huguenot A, et al. (2013) Fe-S cluster biosynthesis controls uptake of aminoglycosides in a ROS-less

death pathway. Science 340: 1583–1587. Available: http://www.sciencemag.org/content/340/6140/1583.abstract. Accessed 29 September 2015.

8. Imlay JA (2013) The molecular mechanisms and physiological consequences of oxidative stress : lessons from a model bacterium. Nat Publ Gr. Available: http://dx.doi.org/10.1038/nrmicro3032.

9. Imlay JA, Linn S (1986) Bimodal pattern of killing of DNA-repair-defective or anoxically grown Escherichia coli by hydrogen peroxide. J Bacteriol 166: 519–527. Available: http://www.ncbi.nlm.nih.gov/pubmed/3516975. Accessed 29 August 2016.

10. Ritz C, Baty F, Streibig JC, Gerhard D (2015) Dose-Response Analysis Using R. PLoS One 10: e0146021. Available: http://dx.plos.org/10.1371/journal.pone.0146021. Accessed 24 May 2018.

11. Halliwell B, Clement MV, Long LH (2000) Hydrogen peroxide in the human body. FEBS Lett 486: 10–13. Available: https://www.sciencedirect.com/science/article/pii/S0014579300021979. Accessed 24 May 2018.

12. Ronin I, Katsowich N, Rosenshine I, Balaban NQ (2017) A long-term epigenetic memory switch controls bacterial virulence bimodality. Elife 6. Available: http://www.ncbi.nlm.nih.gov/pubmed/28178445. Accessed 7 June 2018.

13. Miyaue S, Suzuki E, Komiyama Y, Kondo Y, Morikawa M, et al. (2018) Bacterial Memory of Persisters: Bacterial Persister Cells Can Retain Their Phenotype for Days or Weeks After Withdrawal From Colony–Biofilm Culture. Front Microbiol 9: 1396. Available: https://www.frontiersin.org/article/10.3389/fmicb.2018.01396/full. Accessed 31 July 2018.

14. Veening J-W, Smits WK, Kuipers OP (2008) Bistability, Epigenetics, and Bet-Hedging in Bacteria. Annu Rev Microbiol 62: 193–210. Available: http://www.annualreviews.org/doi/10.1146/annurev.micro.62.081307.163002. Accessed 24 May 2018.

15. Casadesú S J, D ’ari R (n.d.) Memory in bacteria and phage. Available: https://onlinelibrary.wiley.com/doi/pdf/10.1002/bies.10102. Accessed 24 May 2018.

16. Arifuzzaman M, Maeda M, Itoh A, Nishikata K, Takita C, et al. (2006) Large-scale identification of protein-protein interaction of Escherichia coli K-12. Genome Res 16: 686–691. Available: http://www.ncbi.nlm.nih.gov/pubmed/16606699. Accessed 28 November 2017.

17. Gottesman S (2004) THE SMALL RNA REGULATORS OF ESCHERICHIA. Annu Rev Microbiol 58: 303–328. doi:10.1146/annurev.micro.58.030603.123841.

18. Basineni SR, Madhugiri R, Kolmsee T, Hengge R, Klug G (2009) The influence of Hfq and ribonucleases on the stability of the small non-coding RNA OxyS and its target rpoS in E. coli is growth phase dependent. RNA Biol 6: 584–594. Available: http://www.ncbi.nlm.nih.gov/entrez/query.fcgi?cmd=Retrieve&db=PubMed&dopt=Citation&list_uids=20016254.

19. González-Flecha B, Demple B (1999) Role for the oxyS gene in regulation of intracellular hydrogen peroxide in Escherichia coli. J Bacteriol 181: 3833–3836. Available: http://www.pubmedcentral.nih.gov/articlerender.fcgi?artid=93864&tool=pmcentrez&rendertype=abstract. Accessed 21 March 2016.

20. Zhang A, Altuvia S, Tiwari A, Argaman L, Hengge-Aronis R, et al. (1998) The OxyS regulatory RNA represses rpoS translation and binds the Hfq (HF-I) protein. EMBO J 17: 6061–6068. Available: http://www.ncbi.nlm.nih.gov/pubmed/9774349. Accessed 6 October 2016.

21. Altuvia S, Weinstein-Fischer D, Zhang A, Postow L, Storz G (1997) A Small, Stable RNA Induced by Oxidative Stress: Role as a Pleiotropic Regulator and Antimutator. Cell 90: 43–53. Available: http://www.sciencedirect.com/science/article/pii/S0092867400803128. Accessed 16 February 2016.

22. Tjaden B, Goodwin SS, Opdyke JA, Guillier M, Fu DX, et al. (2006) Target prediction for small, noncoding RNAs in bacteria. Nucleic Acids Res 34: 2791–2802. Available: http://www.ncbi.nlm.nih.gov/pubmed/16717284. Accessed 20 April 2018.

23. Barshishat S, Elgrably-Weiss M, Edelstein J, Georg J, Govindarajan S, et al. (2018) OxyS small RNA induces cell cycle arrest to allow DNA damage repair. EMBO J 37: 413–426. Available: http://www.ncbi.nlm.nih.gov/pubmed/29237698. Accessed 20 April 2018.

24. Zheng M, Wang X, Templeton LJ, Smulski DR, LaRossa RA, et al. (2001) DNA microarray-mediated transcriptional profiling of the Escherichia coli response to hydrogen peroxide. J Bacteriol 183: 4562–4570. Available: http://www.ncbi.nlm.nih.gov/pubmed/11443091. Accessed 13 July 2015.

25. Rodríguez-Rojas A, Makarova O, Müller U, Rolff J (2015) Cationic Peptides Facilitate Iron-induced Mutagenesis in Bacteria. PLOS Genet 11: e1005546. Available: http://dx.plos.org/10.1371/journal.pgen.1005546. Accessed 28 March 2018.

26. Abdul-Tehrani H, Hudson AJ, Chang YS, Timms AR, Hawkins C, et al. (1999) Ferritin mutants of Escherichia coli are iron deficient and growth impaired, and fur mutants are iron deficient. J Bacteriol 181: 1415–1428. Available: http://www.pubmedcentral.nih.gov/articlerender.fcgi?artid=93529&tool=pmcentrez&rendertype=abstract. Accessed 18 March 2015.

27. Varghese S, Wu A, Park S, Imlay KRC, Imlay JA (2007) Submicromolar hydrogen peroxide disrupts the ability of Fur protein to control free-iron levels in Escherichia coli. Mol Microbiol 64: 822–830. Available: http://doi.wiley.com/10.1111/j.1365-2958.2007.05701.x. Accessed 24 May 2018.

28. Imlay JA (2015) Transcription Factors That Defend Bacteria Against Reactive Oxygen Species. Annu Rev Microbiol 69: 93–108. Available: http://www.annualreviews.org/doi/10.1146/annurev-micro-091014-104322. Accessed 21 December 2016.

29. Aslund F, Zheng M, Beckwith J, Storz G (1999) Regulation of the OxyR transcription factor by hydrogen peroxide and the cellular thiol-disulfide status. Proc Natl Acad Sci U S A 96: 6161–6165. Available: http://www.ncbi.nlm.nih.gov/pubmed/10339558. Accessed 7 December 2016.

30. Liu Y, Bauer SC, Imlay JA (2011) The YaaA protein of the Escherichia coli OxyR regulon lessens hydrogen peroxide toxicity by diminishing the amount of intracellular unincorporated iron. J Bacteriol 193: 2186–2196. Available: http://www.ncbi.nlm.nih.gov/pubmed/21378183. Accessed 31 August 2018.

31. Ollagnier-De Choudens S, Sanakis Y, Hewitson KS, Roach P, Baldwin JE, et al. (2000) Iron-sulfur center of biotin synthase and lipoate synthase. Biochemistry 39: 4165–4173. Available: http://www.ncbi.nlm.nih.gov/pubmed/10747808. Accessed 31 August 2018.

32. Wang X, Kim Y, Ma Q, Hong SH, Pokusaeva K, et al. (2010) Cryptic prophages help bacteria cope with adverse environments. Nat Commun 1: 147. Available: http://www.nature.com/doifinder/10.1038/ncomms1146. Accessed 31 July 2018.

33. Morgan C, Lewis PD (2006) iMARS - Mutation analysis reporting software: An analysis of spontaneous cII mutation spectra. Mutat Res - Genet Toxicol Environ Mutagen 603: 15–26. doi:10.1016/j.mrgentox.2005.09.010.

34. Kino K, Sugiyama H (2001) Possible cause of G·C→C·G transversion mutation by guanine oxidation product, imidazolone. Chem Biol 8: 369–378. Available:

https://www.sciencedirect.com/science/article/pii/S1074552101000199. Accessed 8 June 2018.

35. Rodríguez-Rojas A, Makarova O, Müller U, Rolff J (2015) Cationic Peptides Facilitate Iron-induced Mutagenesis in Bacteria. PLOS Genet 11: e1005546. Available: http://dx.plos.org/10.1371/journal.pgen.1005546. Accessed 24 May 2018.

36. Hall BM, Ma C-X, Liang P, Singh KK (2009) Fluctuation analysis CalculatOR: a web tool for the determination of mutation rate using Luria-Delbruck fluctuation analysis. Bioinformatics 25: 1564–1565. Available: http://www.pubmedcentral.nih.gov/articlerender.fcgi?artid=2687991&tool=pmcentrez&rendertype=abstract. Accessed 1 May 2014.

37. Frenoy A, Bonhoeffer S (2018) Death and population dynamics affect mutation rate estimates and evolvability under stress in bacteria. PLOS Biol 16: e2005056. Available: http://dx.plos.org/10.1371/journal.pbio.2005056. Accessed 22 June 2018.

38. Rodríguez-Rojas A, Makarova O, Rolff J (2014) Antimicrobials, Stress and Mutagenesis. PLoS Pathog 10. doi:10.1371/journal.ppat.1004445.

39. Galhardo RS, Hastings PJ, Rosenberg SM (2007) Mutation as a Stress Response and the Regulation of Evolvability. Crit Rev Biochem Mol Biol 42: 399–435. Available: http://www.ncbi.nlm.nih.gov/pubmed/17917874. Accessed 22 June 2018.

40. Blázquez J, Couce A, Rodríguez-Beltrán J, Rodríguez-Rojas A, Blazquez J, et al. (2012) Antimicrobials as promoters of genetic variation. Curr Opin Microbiol 15: 561–569. Available: http://www.ncbi.nlm.nih.gov/pubmed/22890188. Accessed 24 May 2013.

41. Ram Y, Hadany L (2012) THE EVOLUTION OF STRESS-INDUCED HYPERMUTATION IN ASEXUAL POPULATIONS. Evolution (N Y) 66: 2315–2328. Available: http://www.ncbi.nlm.nih.gov/pubmed/22759304. Accessed 22 June 2018.

42. Couce A, Guelfo JR, Blázquez J (2013) Mutational spectrum drives the rise of mutator bacteria. PLoS Genet 9: e1003167. Available: http://journals.plos.org/plosgenetics/article?id=10.1371/journal.pgen.1003167. Accessed 27 August 2015.

43. Couce A, Rodríguez-Rojas A, Blázquez J (2015) Bypass of genetic constraints during mutator evolution to antibiotic resistance. Proc Biol Sci 282. doi:10.1098/rspb.2014.2698.

44. Agashe D (2017) The road not taken: Could stress-specific mutations lead to different evolutionary paths? PLOS Biol 15: e2002862. Available: http://www.ncbi.nlm.nih.gov/pubmed/28594832. Accessed 22 June 2018.

45. Datsenko KA, Wanner BL (2000) One-step inactivation of chromosomal genes in Escherichia coli K-12 using PCR products. Proc Natl Acad Sci U S A 97: 6640–6645. Available: http://www.ncbi.nlm.nih.gov/entrez/query.fcgi?cmd=Retrieve&db=PubMed&dopt=Citation&list_uids=10829079.

46. Rappsilber J, Mann M, Ishihama Y (2007) Protocol for micro-purification, enrichment, pre-fractionation and storage of peptides for proteomics using StageTips. Nat Protoc 2: 1896–1906. Available: http://www.ncbi.nlm.nih.gov/pubmed/17703201. Accessed 1 October 2014.

47. Tyanova S, Temu T, Carlson A, Sinitcyn P, Mann M, et al. (2015) Visualization of LC-MS/MS proteomics data in MaxQuant. Proteomics 15: 1453–1456. Available: http://doi.wiley.com/10.1002/pmic.201400449. Accessed 28 November 2017.

48. Pfaffl MW, Horgan GW, Dempfle L (2002) Relative expression software tool (REST) for group-wise comparison and statistical analysis of relative expression results in real-time PCR. Nucleic Acids Res 30: e36. Available: http://www.pubmedcentral.nih.gov/articlerender.fcgi?artid=113859&tool=pmcentrez&rendertype=abstract. Accessed 13 May 2014.

49. Bustin SA, Benes V, Garson JA, Hellemans J, Huggett J, et al. (2009) The MIQE guidelines: minimum information for publication of quantitative real-time PCR experiments. Clin Chem 55: 611–622. Available: http://www.ncbi.nlm.nih.gov/pubmed/19246619. Accessed 29 April 2014.

50. Seemann T (2015) Snippy: fast bacterial variant calling from NGS reads. Available: https://github.com/tseemann/snippy.

51. Li H, Durbin R (2009) Fast and accurate short read alignment with Burrows-Wheeler transform. Bioinformatics 25: 1754–1760. Available: http://www.ncbi.nlm.nih.gov/pubmed/19451168. Accessed 18 May 2018.

52. Garrison E, Marth G (2012) Haplotype-based variant detection from short-read sequencing. Available: https://arxiv.org/pdf/1207.3907.pdf. Accessed 19 May 2018.

53. Deatherage DE, Barrick JE (2014) Identification of Mutations in Laboratory-Evolved Microbes from Next-Generation Sequencing Data Using breseq. Methods in molecular biology (Clifton, N.J.). Vol. 1151. pp. 165–188.

Available: http://www.ncbi.nlm.nih.gov/pubmed/24838886. Accessed 19 May 2018.

54. Sanders LH, Sudhakaran J, Sutton MD (2009) The GO system prevents ROS-induced mutagenesis and killing in Pseudomonas aeruginosa. FEMS Microbiol Lett 294: 89–96. Available: http://www.ncbi.nlm.nih.gov/entrez/query.fcgi?cmd=Retrieve&db=PubMed&dopt=Citation&list_uids=19291074.

55. Rodriguez-Rojas A, Blazquez J (2009) The Pseudomonas aeruginosa pfpI gene plays an antimutator role and provides general stress protection. J Bacteriol 191: 844–850. Available: http://www.ncbi.nlm.nih.gov/entrez/query.fcgi?cmd=Retrieve&db=PubMed&dopt=Citation&list_uids=19028889.

56. R Core Team (2015) R: A language and environment for statistical computing. Vienna, Austria: R Foundation for Statistical Computing.

Figure 1. Hydrogen peroxide killing curves of *E. coli* MG1655. Panel A shows bacterial sensitivity to the 1 mM of hydrogen peroxide. Panel B shows the priming effect or improved response when cells are treated in advanced with a non-lethal dose (0.1 mM). Curves represent the mean of five cultures per time point. Error bars correspond to the standard deviation.

Figure 2. Priming memory decline over time after induction of priming response with H_2O_2 0.1 mM. Each point represents the median of five replications. Error bars indicate the interquartile ranges of the sample. Asterisks indicate significant differences between each time-point pair (Mann–Whitney U test, $p < 0.05$).

Figure 3. Heatmap of relative protein expression based on quantitative lable-free quantification by liquid chromatography/mass spectrometry (LC-MS). Hierarchical clustering of the intensities was performed by using Euclidean distances between means. Row indicate the fluctuation of protein (by gene names) level at 5 minutes after addition of 0.1 and 1 mM H_2O_2. Intensity ranges

963 from highest intensity (green) to lowest (red). Only the most 50 statistically
964 significant upregulated proteins taking as refrence 0.1 mM concentration.
965
966 **Figure 4**. Heatmap of relative protein expression based on quantitative lable-
967 free quantification by liquid chromatography/mass spectrometry (LC-MS).
968 Hierarchical clustering of the intensities was performed by using Euclidean
969 distances between means. Row indicate the fluctuation of protein (by gene
970 names) level at different time points. Intensity ranges from highest intensity
971 (green) to lowest (red). Only the most 50 statistically significant upregulated
972 proteins at time point T1 (30 minutes after priming) are represented to follow
973 their fluctuation in the other time points with 30 minutes between them.
974
975 **Figure 5**. Projection of differentially translated proteins 30 minutes after
976 addition of H_2O_2 on protein-protein interaction network of *E. coli* K12. Pale green
977 nodes indicate upregulated proteins while pale red represents downregulated
978 ones. Note that the most critical nodes (DnaK and GloL) of the protein-protein
979 interaction network are affected. The interactions among nodes show the wide-
980 proteome impact of H_2O_2.
981
982 **Figure 6**. Scatter plot of survival to H_2O_2 of different mutants of *E. coli* MG1655
983 in responsive genes to oxidative stress.
984
985 **Figure 7**. Scatter plot of priming response of different mutants of *E. coli*
986 MG1655 in responsive genes to oxidative stress.
987
988 **Figure 8**. Proportion of population extinctions (20 populations per treatment)
989 due to exposure to growing concentration of H_2O_2. Both, priming and triggering
990 doses were increased twofold daily up to 32 mM, where total extinction was
991 reached. Evolvability differs between the two treatments, naïve and primed
992 populations (Cox's proportional hazard, $p < 0.05$).
993
994 **Figure 9**. Mapping of mutations that are unique to each H_2O_2-evolved
995 populations shared ones. The positions indicate the approximate locations of
996 mutations in the *E. coli* MG1655 chromosome relative to the wild-type. Three
997 generic main type of changes are indicated.

Figure 10. Mutational spectra. Frequencies of different types of mutations among evolved populations of both primed and no-primed conditions. The number of mutations (nucleotide substitutions and indels) is plotted against respective nucleotide positions within the gene fragment. In this analysis, the mutations were taken by type regardless of the targets by generating two frequency tables to compare frequency by type of mutation of evolved populations under priming and non-priming regimes. The mutational spectra are significantly different between the two conditions according to the spectrum analysis software iMARS [32].

Figure S1. Sensitivity of *E. coli* MG1655 to hydrogen peroxide in a multi-well plate experiment. Panel A represents the sensitivity of the strain to growing concentration of H_2O_2 to mid-exponential phase cultures in LB. Panel B represents priming response to 32 mM of hydrogen peroxide 30 minutes after pre-exposure to different priming concentrations. Each point represents the average of eight independent determinations.

Figure S2. Relative gene expression for *E. coli* MG1655 OxyR regulon selected genes in treatments with 0.1 mM H_2O_2 vs. non-treated bacteria. Cells were collected 30 minutes after exposure. Error bars represent the standard error of the mean of three independent biological replicas, each one being the average of three technical repetitions.

Figure S3. OD600 of cells during priming and sampling for proteomic experiments.

Figure S4. Boxplot showing the H_2O_2-induced mutant frequency of naïve and primed (pre-treated with 0.1 mM, 30 minutes in advanced) cultures challenged with 1 mM and plated in rifampicin (100 µg/ml). There is no overlapping of confidence intervals for a confidence of 95% (3.2×10^{-7} to 4.92×10^{-7} for naïve and 1.75×10^{-8} to 5.62×10^{-8} for primed cells). Error bars represent the

interquartile ranges. Both samples are the results of five independent replications.

Figure 1

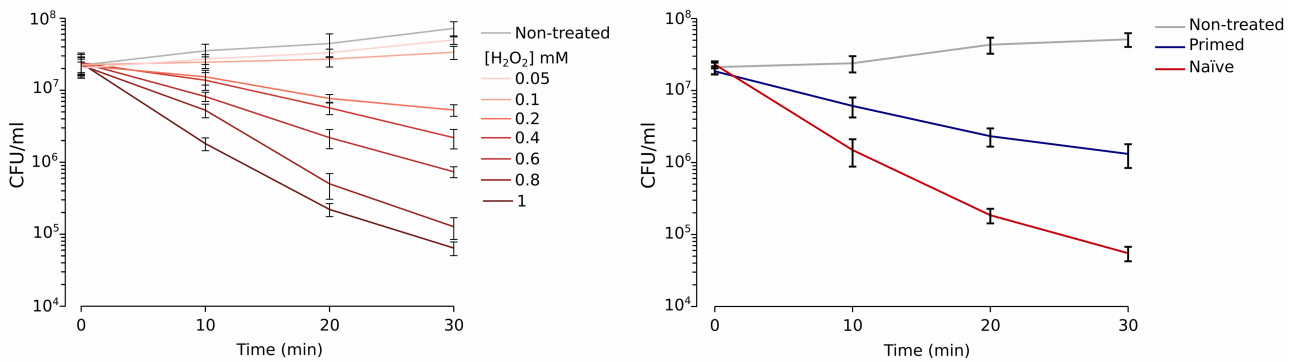

Figure 2

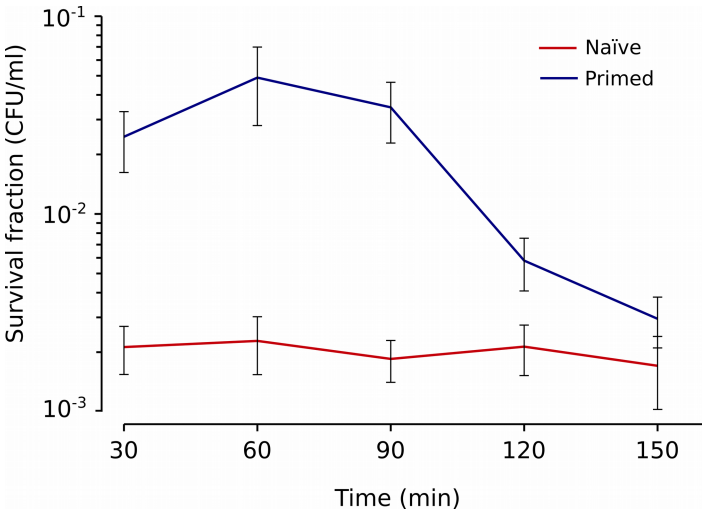

Figure 3

Changes in the 50 most significantly upregulated proteins (by gene names)

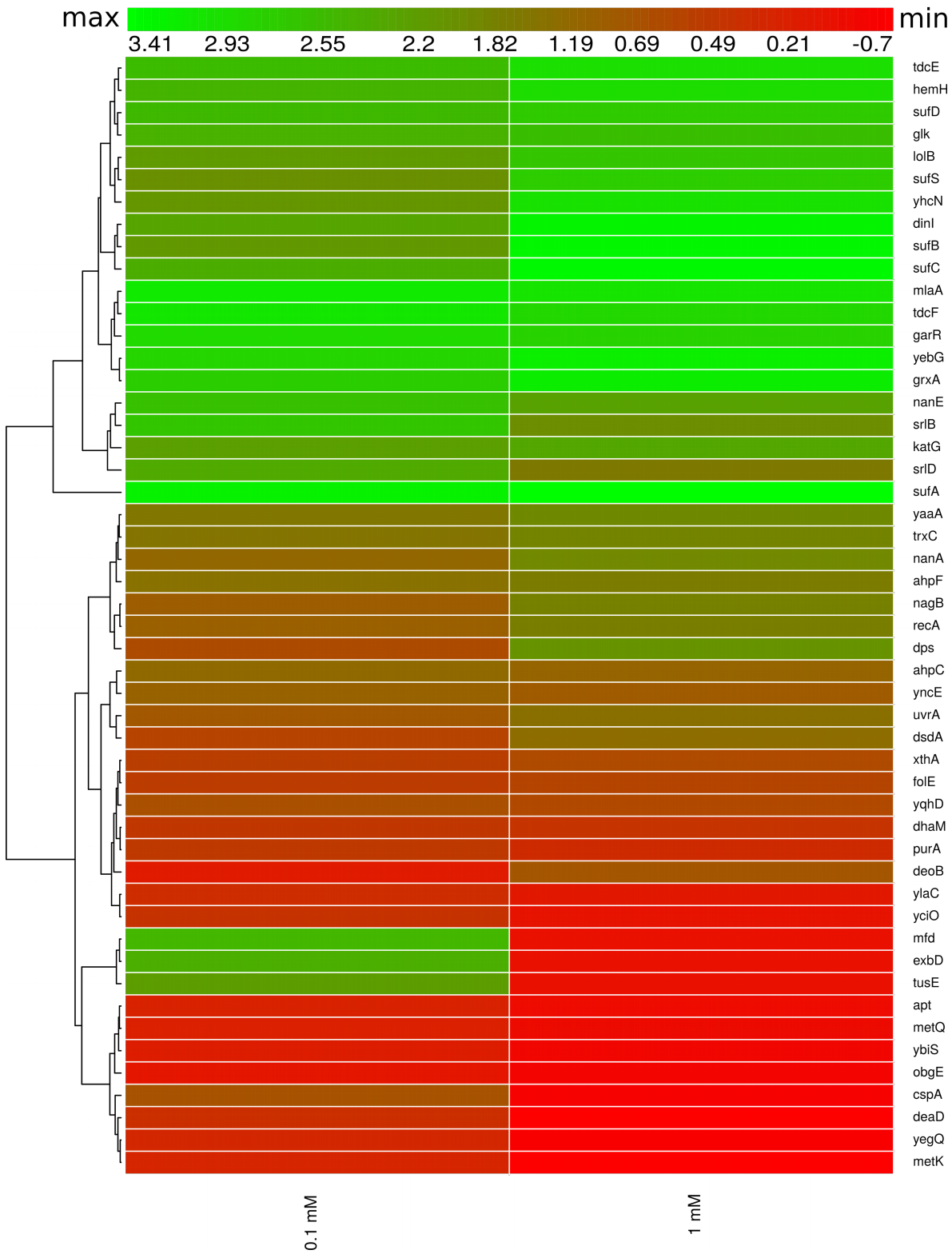

Figure 4

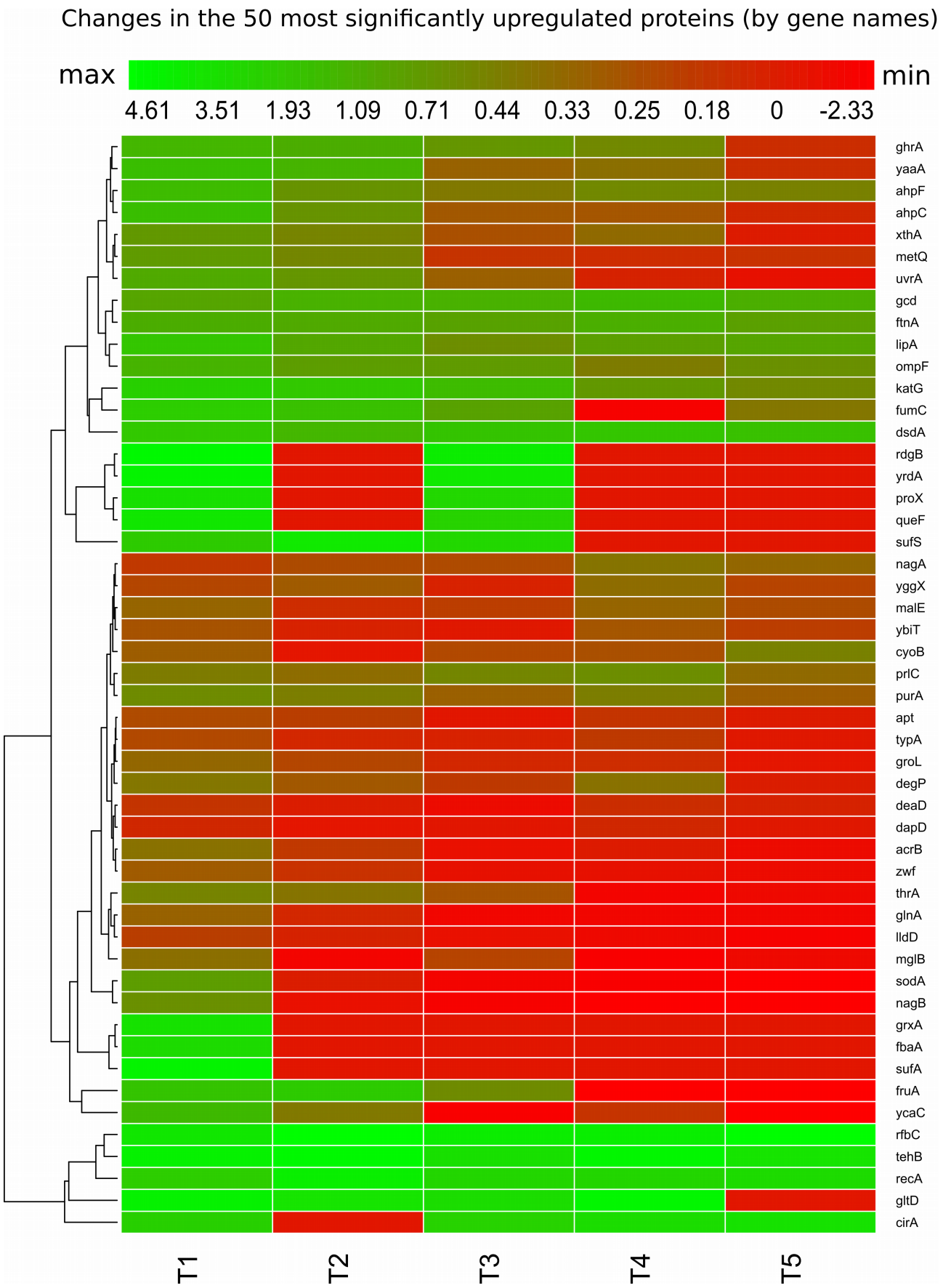
Changes in the 50 most significantly upregulated proteins (by gene names)
max
min
4.61
3.51
1.93
1.09
0.71
0.44
0.33
0.25
0.18
0
-2.33
ghrA
yaaA
ahpF
ahpC
xthA
metQ
uvrA
gcd
ftnA
lipA
ompF
katG
fumC
dsdA
rdgB
yrdA
proX
queF
sufS
nagA
yggX
malE
ybiT
cyoB
prlC
purA
apt
typA
groL
degP
deaD
dapD
acrB
zwf
thrA
glnA
lldD
mglB
sodA
nagB
grxA
fbaA
sufA
fruA
ycaC
rfbC
tehB
recA
gltD
cirA
T1
T2
T3
T4
T5

Figure 5

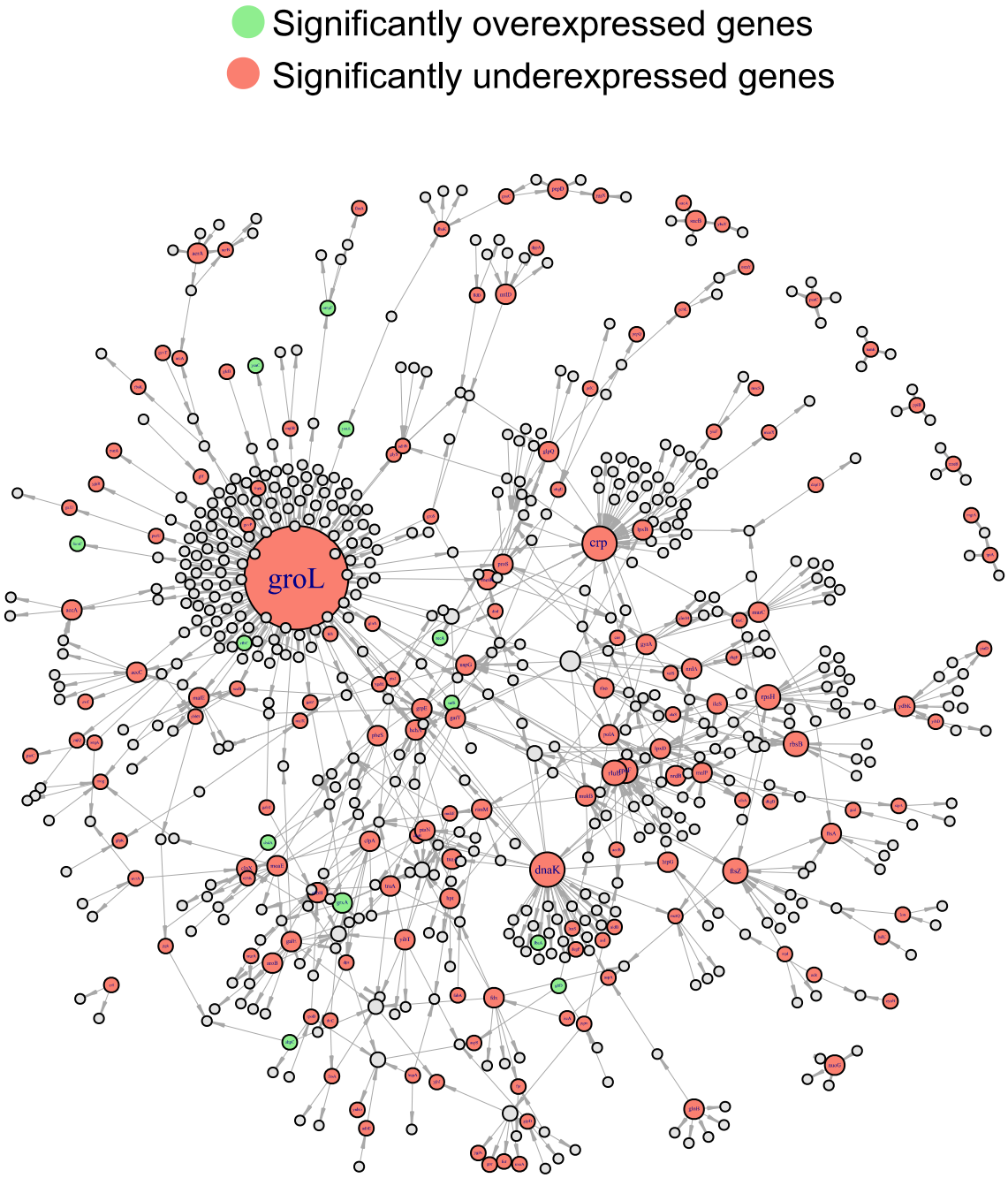
Significantly overexpressed genes
Significantly underexpressed genes
groL
crp
dnaK

Figure 6

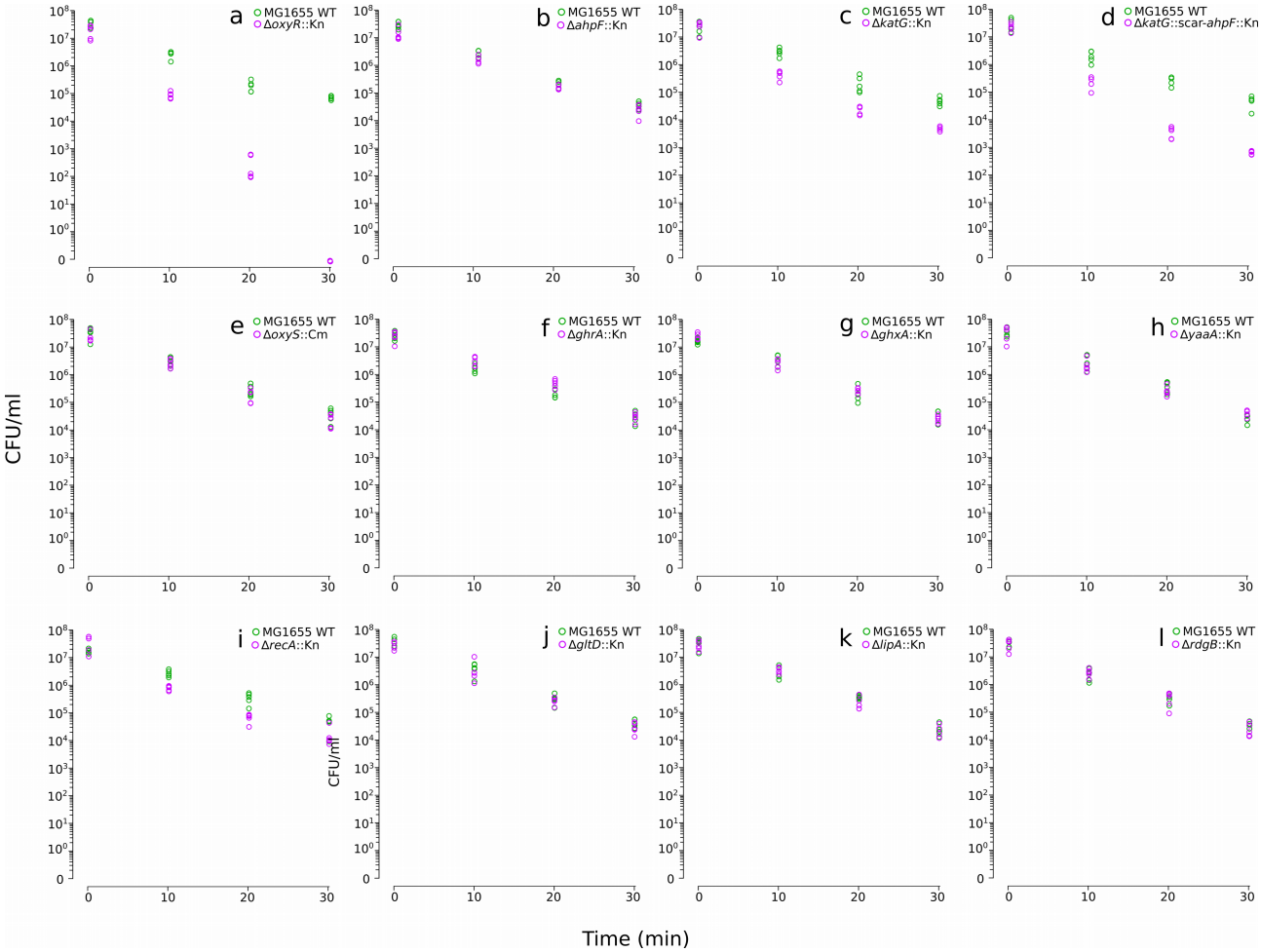

Figure 7

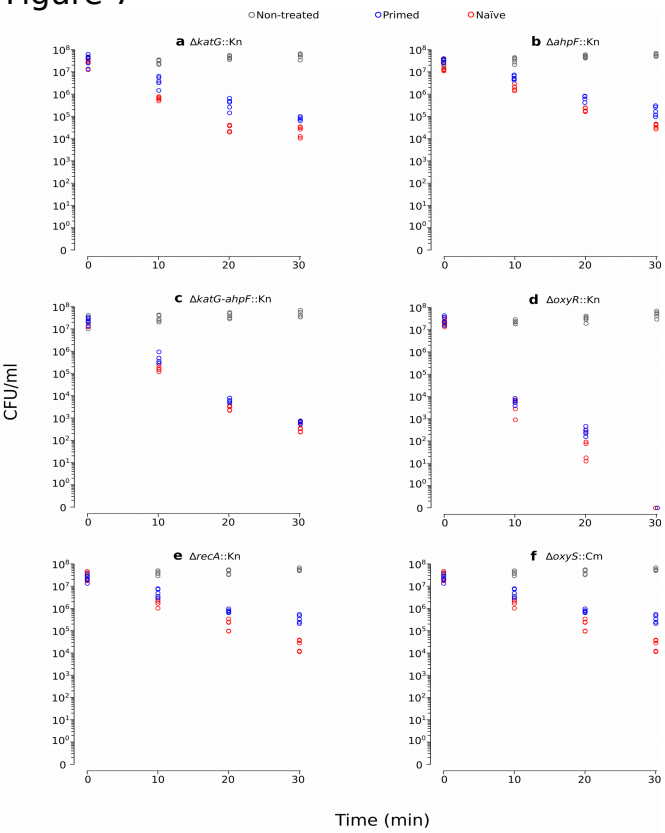

Figure 8

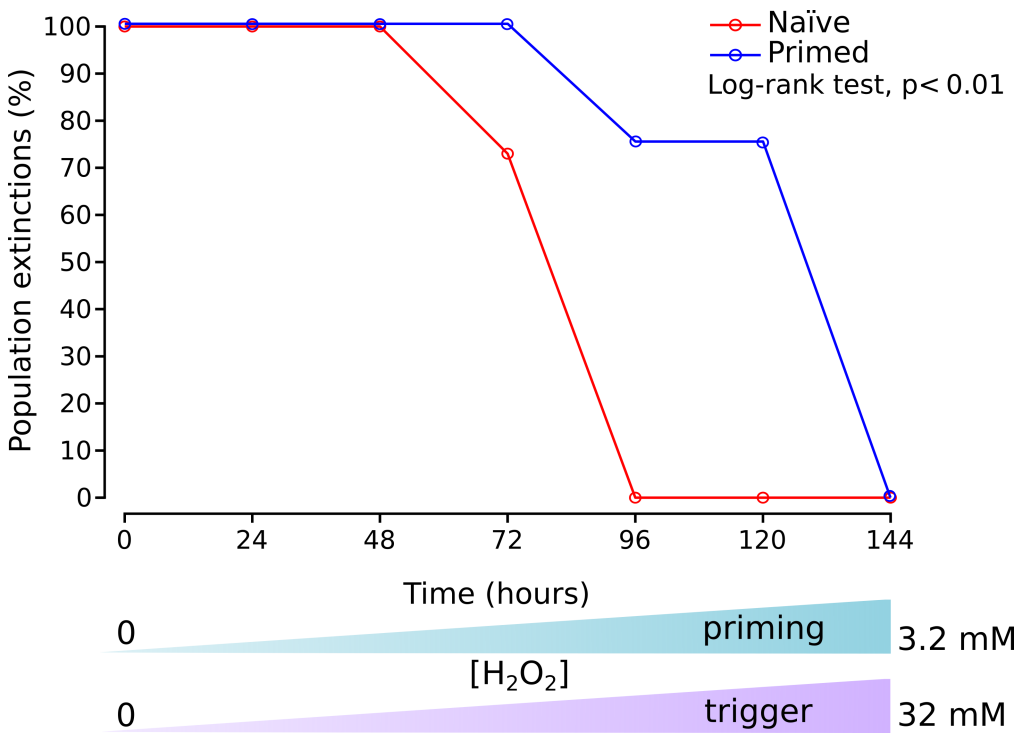
Naïve
Primed
Log-rank test, p< 0.01
Population extinctions (%)
100
90
80
70
60
50
40
30
20
10
0
0
24
48
72
96
120
144
Time (hours)
0
priming
3.2 mM
[H2O2]
0
trigger
32 mM

Figure 9

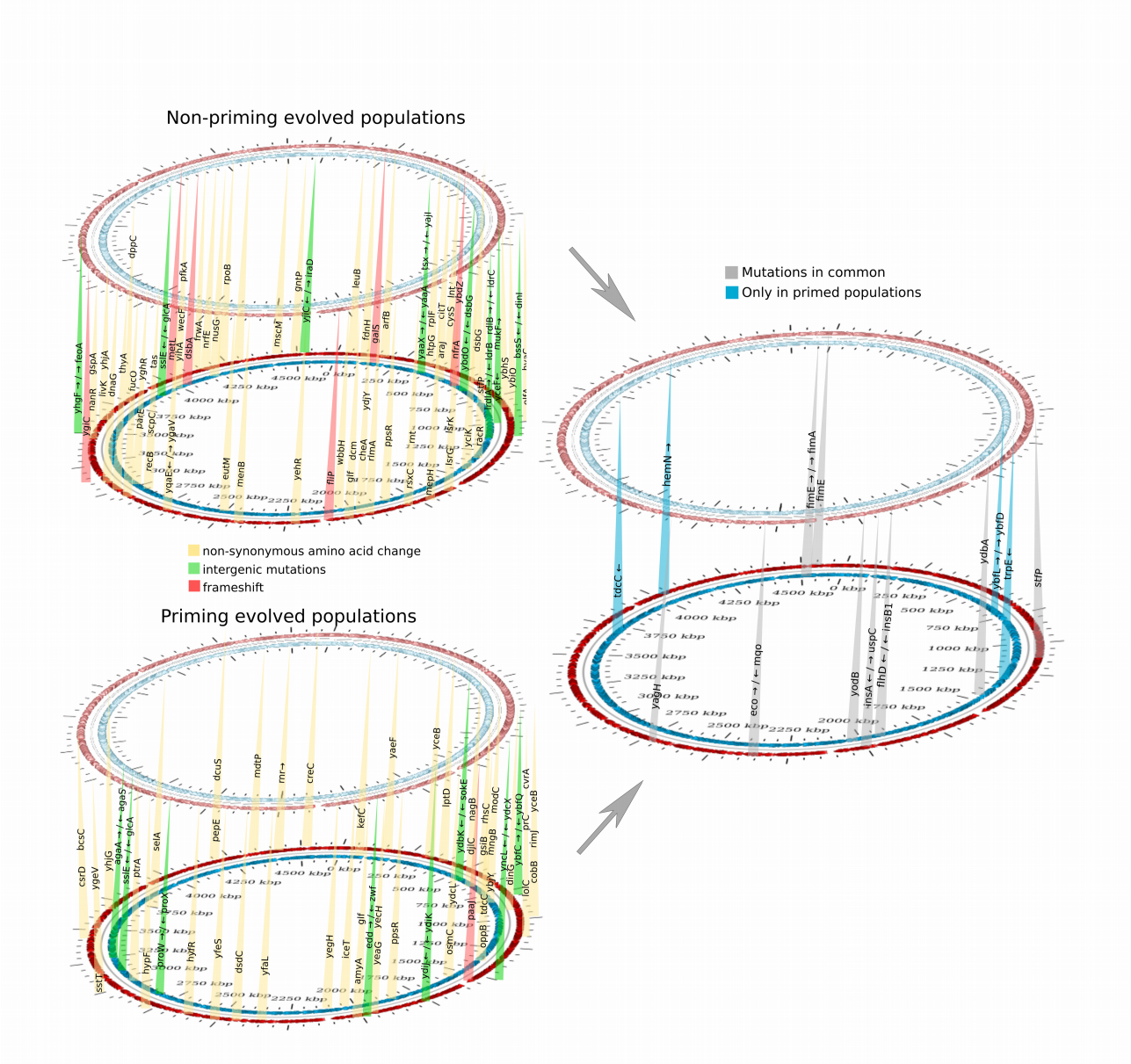
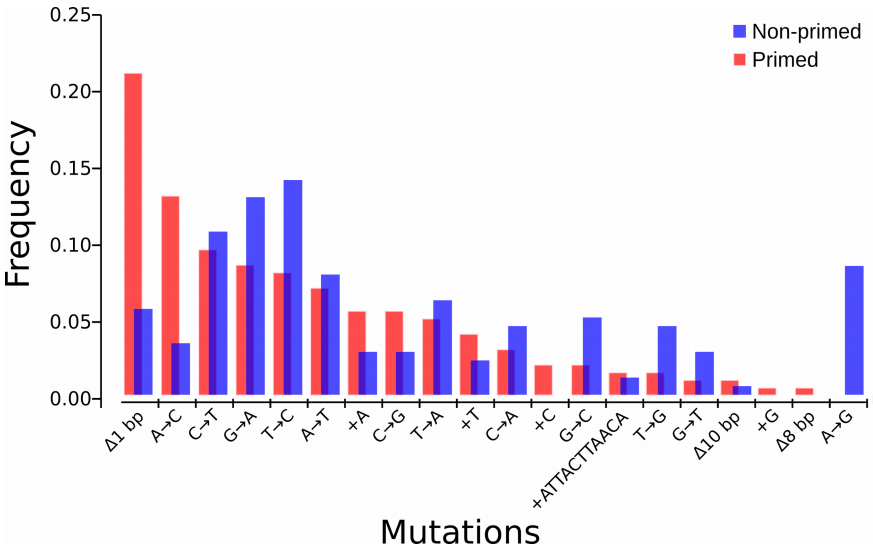
Figure 10